

CP VIOLATION IN NEUTRINO OSCILLATIONS WITHOUT ANTINEUTRINOS: ENERGY DEPENDENCE

Jose Bernabeu and Catalina Espinoza

*Departamento de Fisica Teorica and IFIC, CSIC-University of Valencia,
E-46100, Burjassot, Valencia, Spain*

E-mail: jose.bernabeu@uv.es

m.catalina.espinoza@uv.es

ABSTRACT

The next generation of long baseline neutrino oscillation experiments will aim at determining the unknown mixing angle θ_{13} , the type of neutrino mass hierarchy and CP-violation. We discuss the separation of these properties by means of the energy dependence of the oscillation probability and we consider an hybrid setup which combines the electron capture and the β^+ decay from the same radioactive ion with the same boost. We study the sensitivity to the mixing angle and the CP-phase, the CP discovery potential and the reach to determine the type of neutrino mass hierarchy. The analysis is performed for different boosts and baselines. We conclude that the combination of the two decay channels, with different neutrino energies, achieves remarkable results.

1. What is known, what is unknown

In the past decade, atmospheric ^{1,2)}, solar ^{3,4,5)}, reactor ^{6,7,8)} and long-baseline accelerator ^{9,10)} neutrino experiments have provided compelling evidence for the phenomenon of neutrino oscillations. This has reshaped our understanding of the properties of elementary particles as it implies that neutrinos have mass and mix. The combined data can be described by two mass squared differences, Δm_{31}^2 and Δm_{21}^2 , where $\Delta m_{ji}^2 = m_j^2 - m_i^2$, whose current best fit values are $|\Delta m_{31}^2| = 2.4 \times 10^{-3} \text{ eV}^2$ and $\Delta m_{21}^2 = 7.65 \times 10^{-5} \text{ eV}^2$ ¹¹⁾. The two mixing angles θ_{12} and θ_{23} drive the solar and KamLAND, and atmospheric and accelerator neutrino oscillations, respectively, and are measured to be $\sin^2 \theta_{12} = 0.304$ and $\sin^2 \theta_{23} = 0.50$ ¹¹⁾. The third mixing angle, θ_{13} , is yet undetermined but is known to be small or zero. With available data, θ_{13} is constrained to be ¹¹⁾

$$\sin^2 \theta_{13} < 0.040 \text{ (0.056)} \quad \text{at} \quad 2\sigma \text{ (3}\sigma\text{)} . \quad (1)$$

It is interesting to note that very recently a first hint in favour of $\theta_{13} \neq 0$ has been found ¹²⁾ in a combined analysis of atmospheric, solar and long-baseline reactor neutrino data, with:

$$\sin^2 \theta_{13} = 0.016 \pm 0.010 \quad \text{at} \quad 1\sigma , \quad (2)$$

implying a preference for $\theta_{13} > 0$ at 90% CL. The combination of (2) with other analyses is discussed ¹³⁾ by G. L. Fogli in the present Proceedings.

Although the experimental progress in neutrino physics over the last decade has been conspicuous, many of the fundamental questions surrounding neutrinos still need to be addressed. Understanding of the physics beyond the Standard Model responsible for neutrino masses and mixing requires knowledge of the nature of neutrinos (whether Dirac or Majorana particles), the neutrino mass ordering (normal or inverted), the absolute neutrino mass scale, the value of the unknown mixing angle θ_{13} , and whether CP-symmetry is violated in the lepton sector. It will also be necessary to improve the precision on the known parameters, in particular to measure any deviation from maximal θ_{23} and, if so, to determine its octant.

Some of the issues above will be addressed by a future program of neutrino oscillation experiments^{14,15)}. For flavour oscillations, the unitary diagonalization of the neutrino mass matrix, assuming that the flavour mixing affects the three active light neutrinos only, is given by the PMNS matrix U which connects from mass eigenstate neutrinos to flavour eigenstate neutrinos

$$\begin{bmatrix} \nu_e \\ \nu_\mu \\ \nu_\tau \end{bmatrix} = U \begin{bmatrix} \nu_1 \\ \nu_2 \\ \nu_3 \end{bmatrix}, \quad (3)$$

$$U = \begin{bmatrix} 1 & 0 & 0 \\ 0 & c_{23} & s_{23} \\ 0 & -s_{23} & c_{23} \end{bmatrix} \begin{bmatrix} c_{13} & 0 & s_{13} e^{-i\delta} \\ 0 & 1 & 0 \\ -s_{13} e^{i\delta} & 0 & c_{13} \end{bmatrix} \begin{bmatrix} c_{12} & s_{12} & 0 \\ -s_{12} & c_{12} & 0 \\ 0 & 0 & 1 \end{bmatrix}. \quad (4)$$

U is determined by 3 mixing angles and 1 CP-phase, even if neutrinos are Majorana particles. The two additional Majorana phases would need a $\Delta(L) = 2$ process to become observable, as in Neutrinoless Double Beta Decay.

Nuclear reactors¹⁶⁾ and long baseline experiments using conventional beams¹⁰⁾ will be the first to explore θ_{13} below the current limit and maybe confirm the hint for $\theta_{13} \neq 0$ ¹²⁾. If θ_{13} is close to the present bound imposed by the running and near future experiments, the next generation of superbeams^{17,18)}, an extension of a conventional beam with an upgrade in intensity and detector size, and wide-band beams¹⁹⁾ will probe CP-violation and, for sufficiently long baseline, the neutrino mass hierarchy. For small values of θ_{13} or, if θ_{13} is large but a better precision on the neutrino parameters needs to be achieved, the community must turn to the novel concepts of the neutrino factory^{20,21)} or beta-beam^{22,23)}. Whereas conventional beams sourced from pion decays have an intrinsic contamination of electron neutrino at the $\sim 1\%$ level (owing to kaons in the beam), neutrino factories and beta-beams will have clean sources from highly accelerated muons and ions, respectively, producing a well-collimated beam. In a neutrino factory, muons (antimuons) are produced, cooled and accelerated to a high boost before being stored in a decay ring. The subsequent decay sources a muon neutrino (muon antineutrino) and electron antineutrino (electron neutrino) which are aimed at magnetised detectors located a very long distance from the source. The use

of magnetised detectors is necessary to separate the ‘right muon’ disappearance signal from the ‘wrong muon’ appearance signal, which is sensitive to matter effects and CP-violation. A beta-beam will exploit accelerated ions that β -decay sourcing a clean, collimated, electron neutrino beam. Magnetised detectors will not be necessary in this case, the only requirement being possession of good muon identification to detect the appearance channels. Therefore, water Čerenkov (WC), totally active scintillator, liquid argon detectors and non-magnetised iron calorimeters could be used, depending on the peak energy.

The determination of the oscillation parameters is severely affected by degeneracies: the possibility that different sets of the unknown parameters ($\text{sgn}(\Delta m_{31}^2)$, δ , θ_{13} , θ_{23} octant) can provide an equally good fit to the probability for neutrino and antineutrino oscillations, for fixed baselines and energy. Therefore, a high precision measurement of the appearance probabilities is not sufficient to discriminate the various allowed solutions. In order to weaken or resolve this issue, various strategies have been put forward: exploiting the energy dependence of the signal in the same experiment, using reactor neutrino experiments with an intermediate baseline, combining different long baseline experiments, adding the information on θ_{13} from reactor experiments, or using more than one baseline for the same beam. In addition, θ_{13} controls the Earth matter effects in multi-GeV atmospheric and accelerator neutrino oscillations, as well as in supernovae. These might provide useful information on the type of neutrino mass hierarchy and θ_{13} .

2. CP-violation in neutrino oscillations

The magnitude of the T-violating and CP-violating interference in neutrino oscillation probabilities is directly proportional to $\sin \theta_{13}$ ^{24,25)}. CP-violation can be observed either by an Asymmetry between neutrinos and antineutrinos and/or by Energy Dependence in the neutrino channel. In the last case, the CP phase δ plays the role of a phase shift in the interference pattern between the atmospheric and solar amplitudes for the appearance oscillation probability. This result is a consequence²⁵⁾ of the assumptions of CPT-invariance and No Absorptive part in the oscillation amplitude: the Hermitian character of the Hamiltonian responsible of the time evolution says that the CP-odd=T-odd probability $P(\nu_e \rightarrow \nu_\mu) - P(\bar{\nu}_e \rightarrow \bar{\nu}_\mu)$ is an odd function of time, i.e., an odd function of the baseline L . In vacuum neutrino oscillations for relativistic neutrinos, the oscillation phase depends on the ratio L/E , then the CP-odd term becomes an odd function of the energy E for fixed L . With the same reasoning, the CP-even terms are even functions of the energy E in the oscillation probability. In this way, Energy Dependence in the appearance oscillation probability is able to disentangle CP-even and CP-odd terms.

The explicit expression for the suppressed appearance probability for neutrinos in

vacuum oscillations is given by

$$\begin{aligned}
P(\nu_e \rightarrow \nu_\mu) &= s_{23}^2 \sin^2 2\theta_{13} \sin^2 \left(\frac{\Delta_{13} L}{2} \right) + c_{23}^2 \sin^2 2\theta_{12} \sin^2 \left(\frac{\Delta_{12} L}{2} \right) \\
&+ \tilde{J} \cos \left(\frac{\Delta_{13} L}{2} + \delta \right) \frac{\Delta_{12} L}{2} \sin \left(\frac{\Delta_{13} L}{2} \right), \quad (5)
\end{aligned}$$

where $\Delta_{12} \equiv \Delta m_{21}^2/(2E)$, $\Delta_{13} \equiv \Delta m_{31}^2/(2E)$ and $\tilde{J} \equiv c_{13} \sin 2\theta_{12} \sin 2\theta_{23} \sin 2\theta_{13}$. This expression shows, in fact, that $|U(e3)|$ gives the strength of the probability, whereas δ governs the interference pattern as a phase shift. Furthermore, the separate atmospheric probability, the solar probability and the CP-even term of the interference are even functions of E/L . On the contrary, the CP-odd term of the interference between the atmospheric and solar amplitudes is an odd function of E/L . This result suggests the idea of disentangling δ from $|U(e3)|$ without a need of comparing neutrino and antineutrino events, which have different beam systematics and different cross sections in the detector: either monochromatic neutrino beams with different boosts or a combination of channels with different neutrino energies in the same boost are able of separating the CP-violating phase.

Due to neutrino propagation through the Earth, matter effects can "fake" CP-violation in the sense that the presence of matter affects neutrino and antineutrino oscillations in a different way. It is not easy to disentangle matter effects from CP-violation since there is the so-called "mass hierarchy degeneracy", which swaps the effect of matter for neutrino and antineutrino oscillation according to the sign of Δm_{31}^2 . The energy dependence of the $\nu_e \rightarrow \nu_\mu$ oscillation probability, in presence of matter effects, can be studied from the expression ^{26,27)}

$$\begin{aligned}
P(\nu_e \rightarrow \nu_\mu, L) &= T_{atm} + T_{sol} + T_{int}, \\
T_{atm} &\simeq \sin^2 \theta_{23} \sin^2 2\theta_{13} \left(\frac{\Delta_{13}}{A - \Delta_{13}} \right)^2 \sin^2 \left(\frac{(A - \Delta_{13})L}{2} \right), \\
T_{sol} &= \cos^2 \theta_{23} \sin^2 2\theta_{12} \left(\frac{\Delta_{12}}{A} \right)^2 \sin^2 \left(\frac{AL}{2} \right), \\
T_{int} &= \tilde{J} \frac{\Delta_{12}}{A} \frac{\Delta_{13}}{A - \Delta_{13}} \sin \left(\frac{AL}{2} \right) \sin \left(\frac{(A - \Delta_{13})L}{2} \right) \cos \left(\frac{\Delta_{13}L}{2} + \delta \right), \quad (6)
\end{aligned}$$

where $A \equiv \sqrt{2}G_F \bar{n}_e(L)$ and $\bar{n}_e(L) = 1/L \int_0^L n_e(L') dL'$ is the average electron number density. As seen, the energy dependence induced by the presence of $A \neq 0$ is different in T_{atm} , T_{sol} and in the interference T_{int} and, in fact, different from the energy dependence associated with the CP-even versus the CP-odd separation. On the other hand, the mass hierarchy degeneracy in vacuum is now removed because T_{atm} and T_{int} are now changing under the change of sign of Δm_{31}^2 , although T_{sol} remains the same. All in all, we observe the virtues of studying the neutrino appearance probability as a function of the neutrino energy.

From the current discovery phase of θ_{13} , next generation experiments will hence aim at precision measurements of the $\nu_e \rightarrow \nu_\mu$ oscillation probability. This will require

large underground detectors coupled to more intense and pure neutrino beams. These aspects are being studied within the LAGUNA and EURONu design studies. The knowledge on the possible values of θ_{13} is a necessary input to best optimize the search for CP-violation in the leptonic sector.

The energy dependence of the signal is typically used to extract information on the mass hierarchy and CP-violation. Matter effects increase with baseline and energy suggesting that setups with baselines $L > 600$ km are necessary^{28,29,30)} for the determination of the type of neutrino mass ordering. In beta-beam experiments, such strategies would make use of a proposed upgrade of the CERN Super Proton Synchrotron (SPS) which would equip the accelerator with fast superconducting magnets allowing high boosts and fast ramps. The latter are important to reduce the loss of ions through decay in the acceleration stage. A sister approach to the beta-beam is to use the neutrinos sourced from ions that decay mainly through electron capture (EC)^{31,32,33,34)}. If the electron capture decay is dominated by a single channel, then a monoenergetic electron neutrino beam can be produced this way. In this case, all the beam intensity can be concentrated at the appropriate energy to get the best sensitivity to the oscillation parameters. In order to disentangle the CP violating phase with neutrino beams only, one makes use of the different energy dependence of the CP-even and CP-odd terms in the appearance probability²⁵⁾. Electron capture competes with β^+ -decay when the Q_{EC} -value $> 2m_e$, m_e being the electron mass. With the ions identified in³¹⁾, the use of an upgraded SPS or the Tevatron^a is necessary to source baselines in excess of CERN-Frejus (130 km). We will discuss here also a hybrid³⁵⁾ of these two approaches. By selecting a nuclide with $Q_{\text{EC}} \sim 4$ MeV, we can make use of neutrinos from an electron capture spike and β^+ continuous spectrum simultaneously. Assuming a detector with low energy threshold, the use of such ions allows one to exploit the information from the first and second oscillation maxima with a single beam. The use of the hybrid approach makes it possible to use a monochromatic beam at higher energies and a beta-beam at lower energies. The need for good neutrino energy resolution at the higher energies will therefore be less crucial than for high- γ beta-beam scenarios.

3. A combined beta-beam and electron capture neutrino experiment

In this section we discuss the idea³⁵⁾ of the beta-beam and electron capture hybrid approach. We present the spectra of the two branches, their ratio and consider two nuclides which have desirable properties.

The beta-beam is a proposal, originally put forward by P. Zucchelli²²⁾, to accelerate and then store β -emitting ions, which subsequently decay to produce a well collimated, uncontaminated, electron neutrino (or antineutrino) beam. The high lu-

^aNote that the present Tevatron configuration does not ramp fast enough, resulting in a high loss of ions, so this might not be a very realistic experimental setup, at least in the present configuration.

minisities required to achieve a useful physics reach point towards ions with small charge to minimise space charge and half-lives ~ 1 second to reduce ion losses during the acceleration stage whilst maintaining a large number of useful decays per year. The most promising candidate ions are ^{18}Ne and ^8B for neutrinos, and ^6He and ^8Li for antineutrinos. A variant on the beta-beam idea is the use of electron capture to produce monoenergetic neutrino beams. Electron capture is the process in which an atomic electron is captured by a bound proton of the ion $A(Z, N)$ leading to a nuclear state of the same atomic number A , but with the exchange of the proton by a neutron and the emission of an electron neutrino,

$$A(Z, N) + e^- \rightarrow A(Z - 1, N + 1) + \nu_e . \quad (7)$$

The idea of using this process in neutrino experiments was independently discussed in Refs. ^{31,33}). In Ref. ³⁴), ions with low Q_{EC} -value and long half-life, such as ^{110}Sn , were proposed to be accelerated to very high boosts with the LHC. Baselines of 250 km and 600 km were considered with the spectral information coming from the position of the events in the detector. Sensitivities comparable to a Neutrino Factory were obtained for a single boost. However, in order for electron capture machines to become operational, nuclei with shorter half-life are required. The recent discovery of nuclei far from the stability line with kinematically accessible super-allowed spin-isospin transitions to giant Gamow-Teller resonances (see, for example, Ref. ³⁶) opens up such a possibility. The rare-Earth nuclei above ^{146}Gd have a short enough half-life to allow electron capture processes in the decay ring, in contrast to fully-stripped long-lived ions ^{33,34}). This was the scenario put forward in Ref. ³¹) where the use of short-lived ions with Q_{EC} -values around 1-4 MeV was proposed. Machines such as the SPS, an upgraded SPS and the Tevatron could then be used for the acceleration. The ion ^{150}Dy , with Q_{EC} -value 1.4 MeV, was investigated for the CERN-Frejus (130 km) and CERN-Canfranc (650 km) baselines and different boost factors. It was found to have very good physics reach ^{31,32}). Owing to the monochromatic nature of the beam, multiple boosts are necessary to resolve the intrinsic degeneracy in this case.

In the following, we demonstrate how the flux for the electron capture/beta-beam can be built up by discussing them separately and comparing branching ratios. Let the mass difference between the parent and the daughter atoms, $\Delta M_A^{\beta^+} = M_A(Z, N) - M_A(Z - 1, N + 1)$, include the mass and the binding energy of an atomic electron as well. For electron capture, the maximum kinetic energy release is thus given by $Q_{\text{EC}} = \Delta M_A^{\beta^+}$. For β^+ -decay, however, the final atom has an excess electron since a positron is produced. The maximum kinetic energy release is thus given by $Q_{\beta^+} = \Delta M_A^{\beta^+} - 2m_e$. Clearly for $(\Delta M_A^{\beta^+} =) Q_{\text{EC}} < 2m_e$, electron capture is the only allowed process for a proton-rich nucleus. For $Q_{\text{EC}} > 2m_e$, electron capture and positron emission compete, their branching ratios dependent on Q_{EC} . If decay through α emission is also allowed, it is important that this has a relatively low

Q -value so as not to be the dominant channel ^b. For a number of useful ion decays per year N_{ions} , the electron capture neutrino flux is given by ^{31,32)}

$$\frac{d\Phi_{\text{EC}}^{\text{lab}}}{d\Omega dE_\nu} = \frac{\Gamma}{\Gamma_{\text{tot}}} \frac{N_{\text{ions}}}{\pi L^2} \gamma^2 \delta(E_\nu - 2\gamma E_0^{\text{EC}}) \quad (8)$$

for each decay channel. Here, L is the baseline, γ is the Lorentz boost, E_0^{EC} ($= Q_{\text{EC}}$) is the neutrino energy in the ion rest frame and E_ν is the neutrino energy in the lab frame.

The flux for the β -spectrum is found in the usual way. In the rest frame of the ion, the electron neutrino flux is proportional to

$$\frac{d\Phi_\beta^{\text{rf}}}{d\cos\theta dE_{\text{rf}}} \sim E_{\text{rf}}^2 (E_0^\beta - E_{\text{rf}}) \sqrt{(E_{\text{rf}} - E_0^\beta)^2 - m_e^2}. \quad (9)$$

Here, E_0^β ($= Q_{\beta^+} + m_e = Q_{\text{EC}} - m_e$) is the total end-point energy of the decay. The neutrino flux per solid angle at the detector located at distance L from the source after boost γ is ³⁷⁾

$$\left. \frac{d\Phi_\beta^{\text{lab}}}{d\Omega dy} \right|_{\theta \simeq 0} \simeq \frac{N_{\text{ions}}}{\pi L^2} \frac{\gamma^2}{g(y_e)} y^2 (1-y) \sqrt{(1-y)^2 - y_e^2}, \quad (10)$$

where $0 \leq y = \frac{E_\nu}{2\gamma E_0^\beta} \leq 1 - y_e$, $y_e = m_e/E_0^\beta$, and

$$g(y_e) \equiv \frac{1}{60} \left\{ \sqrt{1 - y_e^2} (2 - 9y_e^2 - 8y_e^4) + 15y_e^4 \log \left[\frac{y_e}{1 - \sqrt{1 - y_e^2}} \right] \right\}. \quad (11)$$

Similarly to the case of electron capture, a neutrino with energy E_{rf} in the rest frame will have a corresponding energy $E_\nu = 2\gamma E_{\text{rf}}$ in the laboratory frame along the $\theta = 0^\circ$ axis.

All the known nuclear structure information on the $A = 148$ and $A = 156$ nuclides has been reviewed in Ref. ³⁸⁾ and Ref. ³⁹⁾, respectively, where the information obtained in various reaction and decay experiments is presented, together with adopted level schemes. Currently, a systematic study of electron capture decays in the region of ^{146}Gd , relevant for monoenergetic neutrino beams, is being carried out ⁴⁰⁾. Here, we consider two nuclides, $^{156}_{70}\text{Yb}$ and $^{148m}_{65}\text{Tb}$, that decay through electron capture and β^+ -decay with similar branching ratios whose lifetimes are not too long or too short. Their decays are summarised in Tables 1 and 2. Ytterbium is a nuclide $^{156}_{70}\text{Yb}$ with spin-parity 0^+ , which decays 90% via electron capture plus β^+ -decay ³⁹⁾, with 38% via electron capture and 52% via β^+ -decay ⁴⁰⁾. The remaining 10% goes into

^bThe α decay branching ratio is strongly dependent on the Q_{EC} -value. For low Q_{EC} , the α decay probability is sufficiently long as to allow the weak decay modes to be the main channels.

Decay	Daughter	Neutrino energy (MeV)	BR
β^+	$^{156}_{69}\text{Tm}^*$	2.44 (endpoint)	52%
EC	$^{156}_{69}\text{Tm}^*$	3.46	38%
α	$^{152}_{68}\text{Er}$		10%

Table 1: Decay summary for $^{156}_{70}\text{Yb}$. The Q_{EC} -value for the transition between ground states is 3.58 MeV and taking into account the excitation energy of the final nuclear state (0.12 MeV), the effective $Q_{\text{EC}}^{\text{eff}}$ -value is 3.46 MeV.

Decay	Daughter	Neutrino energy (MeV)	BR
β^+	$^{148}_{64}\text{Gd}^*$	2.05 (endpoint)	32%
EC	$^{148}_{64}\text{Gd}^*$	3.07	68%

Table 2: Decay summary for $^{148m}_{65}\text{Tb}$. The Q_{EC} -value for the transition between ground states is 5.77 MeV and the effective $Q_{\text{EC}}^{\text{eff}}$ -value to the excited state is 3.07 MeV.

α -particles and a different final state. This relatively small branching ratio into α 's helps the nuclide to have a short enough half-life, 26.1 seconds. It is important to note that this electron capture- β^+ -decay transition has only one possible daughter state with spin-parity 1^+ , i.e., it is a Gamow-Teller transition into an excited state of Thulium, $^{156}_{69}\text{Tm}^*$. The transition Q_{EC} -value is ^c Q_{EC} -value = 3.58 MeV. However, the excitation energy of the final nuclear state (0.12 MeV) needs to be taken into account and thus, the effective Q_{EC} -value (difference in the total kinetic energies of the system after and before the decay) is 3.46 MeV ³⁹⁾. The electron capture energy of ~ 4 MeV is well suited to the intermediate-baselines of Europe and the USA with the available technology, or those available with future upgrades. On the other hand, the $^{148m}_{65}\text{Tb}$ isomer with spin-parity 9^+ has a Q_{EC} -value of 5.77 MeV ^{38,41)}. Although the decay to the ground state of $^{148}_{64}\text{Gd}$ is highly forbidden, the presence of a Gamow-Teller resonance allows the decay into an excited state with effective Q -value 3.07 MeV ⁴²⁾. This nuclide is longer lived than $^{156}_{70}\text{Yb}$ (with a half-life of 2.2 minutes) and will require slightly higher boosts. It is still well suited to intermediate baselines. However, the dominance of the electron capture over the β^+ -decay channel makes this nuclide less desirable. The count rate will be dominated by the single energy of the electron capture which provides insufficient information to obtain the good sensitivities aspired to by future long baseline experiments. It was shown in Refs. ^{31,32)} that two runs with different boosts are necessary for an exclusive or dominant electron capture channel to break the intrinsic degeneracy and achieve good CP-violation discovery. Hence, in what follows we will study this hybrid approach focusing on ^{156}Yb .

^c Q_{EC} -values are typically calculated between ground states unless stated otherwise.

Machine	γ_{\max}	$2\gamma_{\max}Q_{\text{EC}}^{\text{eff}}(\text{GeV})$	$2\gamma_{\max}Q_{\beta^+}^{\text{eff}}(\text{GeV})$
SPS	166	1.15	0.81
Upgraded SPS	369	2.55	1.80

Table 3: Maximum boosts and neutrino endpoint energies for ^{156}Yb available for the current SPS setup and a proposed 1 GeV upgraded SPS.

4. Choice of the boost and baseline

We consider the use of a neutrino beam sourced from boosted ^{156}Yb ions directed along a single baseline. As described above, both the electron capture and β^+ -decay channels are to an excited state of ^{156}Tm with a Q_{EC} -value of 3.46 MeV. In order to fully exploit the electron capture decay mode, the nuclides cannot be fully stripped; at least 16 electrons being left on the ion $^{43})$. The maximum boost, γ_{\max} , available is thus

$$\gamma_{\max} = \frac{E_{\text{acc}}}{m_p} \frac{Z - 16}{A}, \quad (12)$$

where m_p is the mass of the proton and E_{acc} is the maximum energy accessible with the accelerator. Current and future accelerator facilities would be an ideal production environment. In this analysis, we consider the maximum boosts available from the current SPS and upgraded SPS (see Table 3) for the following baselines:

1. Boost $\gamma = 166$ with current SPS

- CERN-Frejus (130 km)
- CERN-Canfranc (650 km)

2. Boost $\gamma = 369$ with an upgraded SPS

- CERN-Canfranc (650 km)
- CERN-Boulby (1050 km)

With the current magnetic rigidity of the SPS, the electron capture spike can be placed on first oscillation for the CERN-Canfranc baseline (650 km) with the beta-beam spectrum peaking around the second oscillation maximum (see Fig. 1). For the upgraded SPS, with proton energy at 1 TeV, the first oscillation maximum and most of the second oscillation are covered for the CERN-Boulby baseline (1050 km).

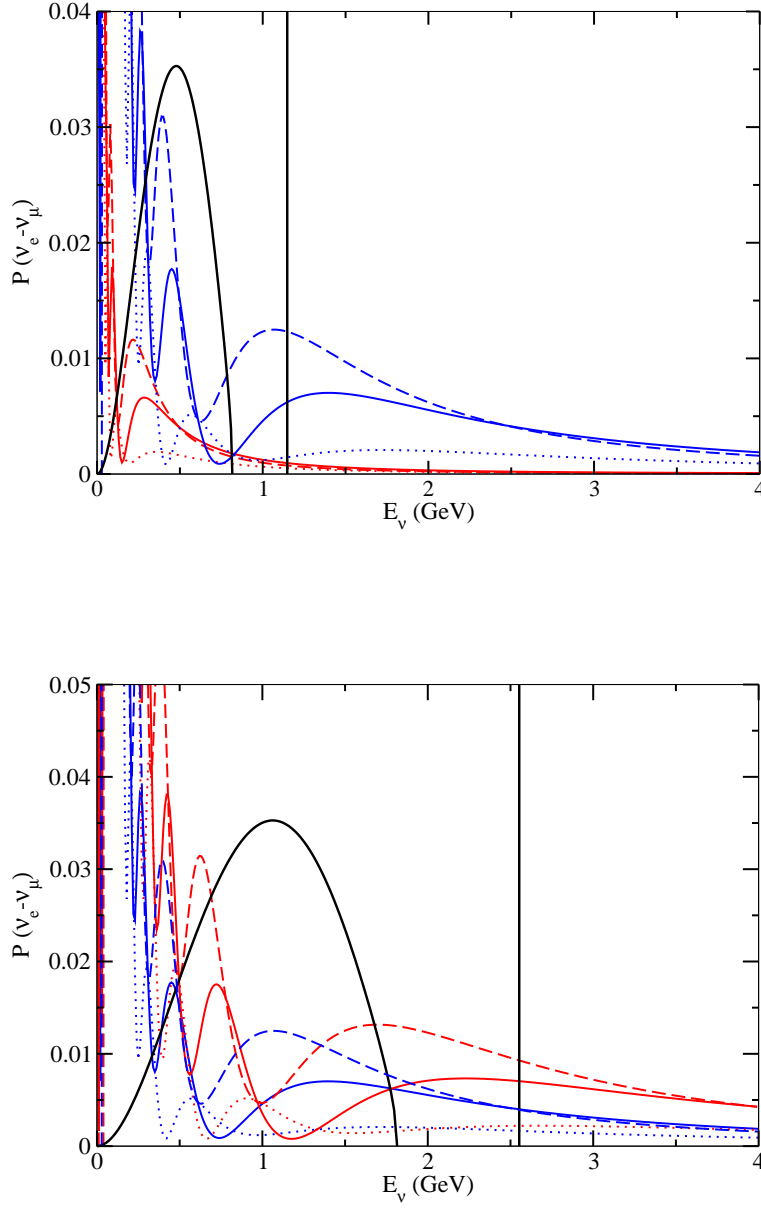


Figure 1: *Top panel:* $\nu_e \rightarrow \nu_\mu$ appearance probabilities for the CERN-Frejus (130 km) and CERN-Canfranc (650 km) baselines. The unoscillated ν_e flux in the laboratory frame is shown for ^{156}Yb given a boost $\gamma = 166$ in arbitrary units. *Bottom panel:* $\nu_e \rightarrow \nu_\mu$ appearance probabilities for the CERN-Canfranc (650 km) and CERN-Boulby (1050 km) baselines. The flux from a boost $\gamma = 369$ is shown in arbitrary units. In both cases, the blue lines correspond to CERN-Canfranc; the red being CERN-Frejus (top panel) and CERN-Boulby (bottom panel). The solid lines correspond to $\delta = 0^\circ$, dashed $\delta = 90^\circ$ and dotted $\delta = -90^\circ$. The value $\sin^2 2\theta_{13} = 0.01$ was taken for all curves.

5. Results

We will compare the physics reach for different experimental Setups, defined by the following:

1. 50 kton detector (LAr or TAsD) with 2×10^{18} ions/yr

- Setup I: CERN-Frejus (130 km) and $\gamma = 166$
- Setup II: CERN-Canfranc (650 km) and $\gamma = 166$
- Setup III: CERN-Canfranc (650 km) and $\gamma = 369$
- Setup IV: CERN-Boulby (1050 km) and $\gamma = 369$

2. 0.5 Mton water-Čerenkov detector with 2×10^{18} ions/yr

- Setup III-WC: CERN-Canfranc (650 km) and $\gamma = 369$
- Setup IV-WC: CERN-Boulby (1050 km) and $\gamma = 369$

I and II correspond to present SPS energies for the boost, whereas III and IV need an upgraded SPS with proton energy 1 TeV. The difference between III(IV) and III(IV)-WC is in the detector. In the first case, we consider a 50 kton detector, like LiAr or TAsD, with energy reconstruction and neutrino spectral information. In the second case, a 0.5 Mton Water Čerenkov detector with neutrino energy from QE events only plus inelastic events in a single bin, with 70% efficiency. Whereas in the first case we use then the total cross section at each energy, for the WC detector we use the total cross section at the EC spike, the QE cross section at each energy bin and the inelastic cross section for a single bin in the β^+ spectrum.

The separation between the energy of the EC spike and the end point energy of the beta-spectrum is possible: if $E_\nu(\text{QE}) > 2\gamma E_0^\beta$, since $E_\nu^{\text{true}} \geq E_\nu(\text{QE})$, the event has to be attributed to the EC flux and, hence, it is not necessary to reconstruct the true neutrino energy.

5.1. Comparing baselines

For this comparison, we take the combined beta-beam and EC fluxes with $\theta_{13} = 1^\circ$ and $\delta = 90^\circ$ for Setups I and II, with different baselines. The result is shown in Fig. 2, where we see that the longer baseline (650 km) is necessary in order to separate the mixing parameter and the CP phase. Violation of CP can be established, only in the last case, for a limited range of values of the parameters.

In fact, the beta-beam channel contributes very little to the overall sensitivity of the setup. This is due to the energy dependence of the flux. The smaller flux,

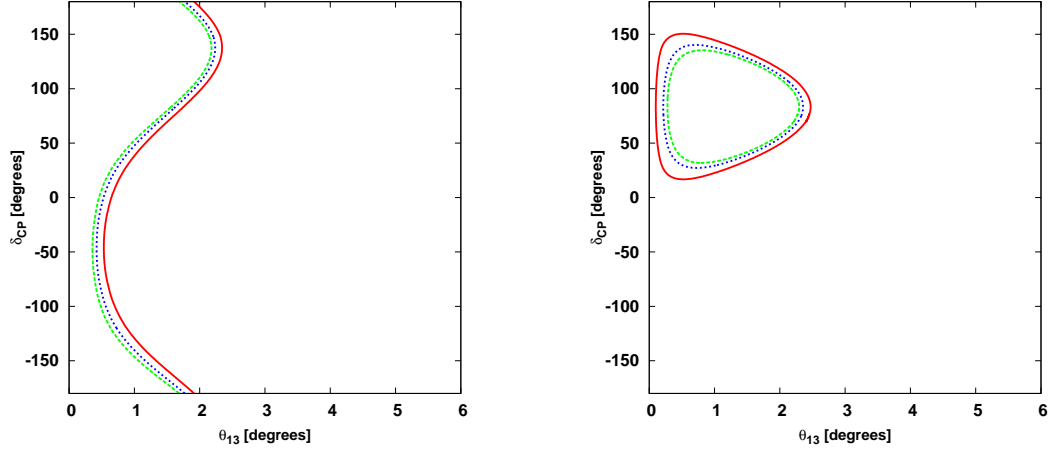


Figure 2: 90%, 95% and 99% CL contours for setup I (left panel) and setup II (right panel). The parameters $\theta_{13} = 1^\circ$ and $\delta = 90^\circ$ have been taken assuming normal mass ordering and $\theta_{23} = 45^\circ$.

combined with the smaller cross section at the energies centred on second oscillation maximum, supplies a scarce count rate. The bulk of the sensitivity is due, in this case, to the electron capture channel, placed on first oscillation maximum, as seen in Fig. 1.

5.2. Comparing boosts at the same baseline

We are going to compare the results for the setups II and III. In going from $\gamma = 166$ to $\gamma = 369$, the electron capture beam is placed in the tail of first oscillation maximum. This gives the beta-beam coverage of the second oscillation maximum and substantial portions of the first oscillation maximum. Then the roles of electron capture and beta-beam are reversed. The beta-beam now contributes much more to the sensitivity as it provides substantial information from the first oscillation maximum and a much higher count rate from the second oscillation maximum.

In Fig. 3 we show the 90%, 95% and 99% CL contours for setups II and III with mixing $\theta_{13} = 1^\circ$ and $\delta = 90^\circ$, using the combination of beta-beam and EC fluxes. We conclude that the sensitivity is better with the upgraded SPS energy.

5.3. The virtues of combining energies from beta-beam and EC

The full power of the combination between the beta-beam spectrum and the EC channel is best illustrated in Fig. 4. For Setup III, we give the results with $\theta_{13} = 3^\circ$ and $\delta = 90^\circ$ for the contribution of the beta-beam, for that of the EC channel and for the combination. Each of the two techniques separately suffer from a continuum of solutions. In fact, the shapes of the allowed regions can be understood by looking at the form of the oscillation probability. The power of the combination of the two

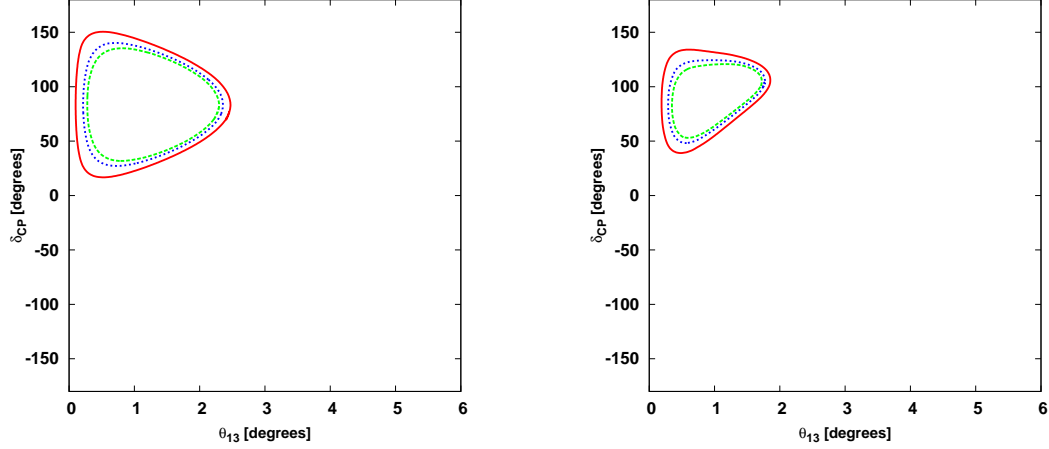


Figure 3: 90%, 95% and 99% CL contours for setup II (left panel) and setup III (right panel). The parameters $\theta_{13} = 1^\circ$ and $\delta = 90^\circ$ have been taken assuming normal mass ordering and $\theta_{23} = 45^\circ$.

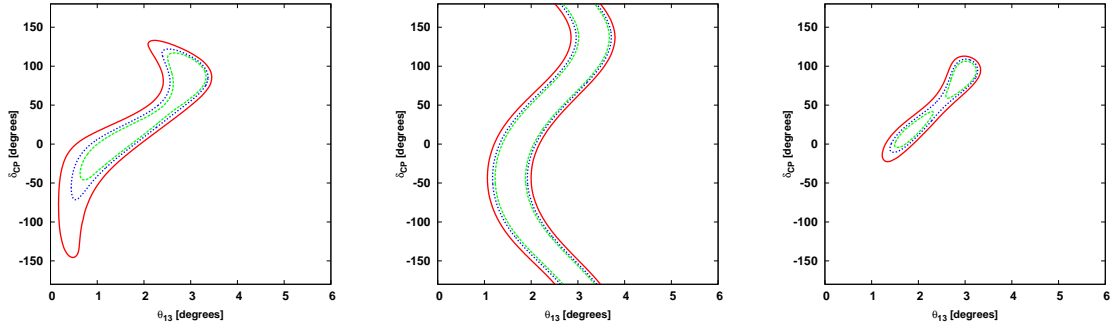


Figure 4: 90%, 95% and 99% CL contours for the setup III, simulated for $\theta_{13} = 3^\circ$ and $\delta = 90^\circ$ assuming normal mass ordering and $\theta_{23} = 45^\circ$. The left panel is the contribution of the beta-beam, the middle panel is for the electron capture channel with the right panel being the combination.

channels under the same conditions is in the difference in phase and in amplitude between the two fake sinusoidal solutions, selecting a narrow allowed region in the parameter space, much more constrained than the two separate techniques.

The marked difference between the beta-beam alone and the combination with the electron capture in this case demonstrate the importance of data from the high energies.

5.4. Disentangling θ_{13} and δ

In Fig. 5, we show the physics reach for setup III-WC, with the effects of the hierarchy clone solution taken into account. From a comparison of Figs. 4 and 5, the increase in event rates improves the results substantially, although not as much as the size factor between the two detectors. However, owing to the relatively short distance, $L = 650$ km, the mass ordering can be determined only for large values of

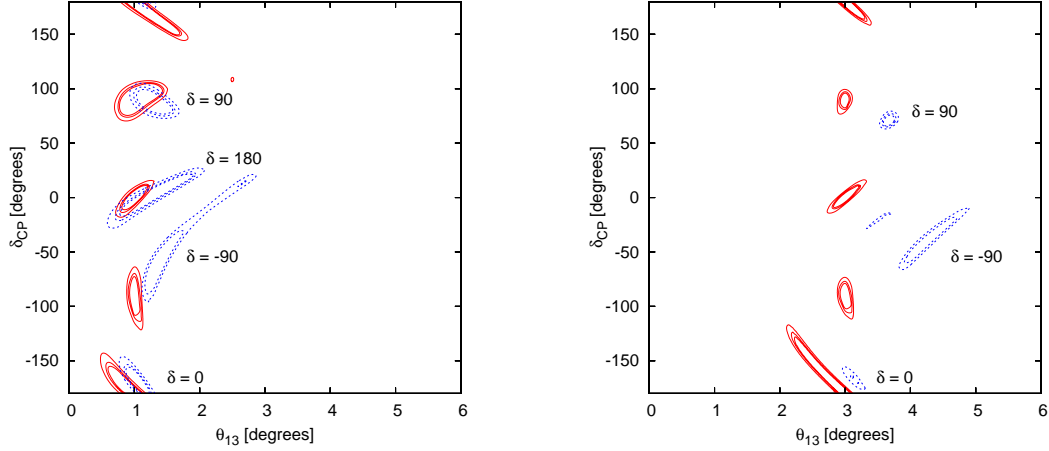


Figure 5: 90%, 95% and 99% CL contours for setup III-WC with solutions from discrete degeneracies included for $\theta_{13} = 1^\circ$ (left panel) and $\theta_{13} = 3^\circ$ (right panel) for different values of the CP-phase, $\delta = -90^\circ, 0^\circ, 90^\circ, 180^\circ$.

the mixing angle θ_{13} . The hierarchy degeneracy worsens the ability to measure θ_{13} and δ with good precision, especially for negative true values of δ . We conclude that a baseline $L = 650$ km, at least, is needed to disentangle the CP phase.

6. CP-violation discovery potential

We now consider the comparison of setups III-WC and IV-WC for the separation of the CP phase δ . Boulby provides a longer baseline $L = 1050$ km than Canfranc $L = 650$ km. This has two contrasting effects on the sensitivity to measure CP-violation: i) Sufficient matter effects to resolve the hierarchy degeneracy for small values of θ_{13} ; ii) It decreases the available statistics.

From Fig. 6, we see that the smaller count rate results in a poorer resolution for the longer baseline. However, the longer baseline allows for a good determination of the mass ordering, thus eliminating more degenerate solutions.

In Fig. 7 we give the CP-violation discovery potential for these two setups. Comparing the two locations of the detector, we notice that the shorter baseline (CERN-Canfranc) has a slightly (significantly) better reach for CP-violation at positive (negative) values of δ than the longer baseline (CERN-Boulby). The longer option, however, performs slightly better at negative δ if the hierarchy is known to be normal and significantly better if the ordering is not determined. This is because the longer baseline can identify the neutrino mass hierarchy for these values of θ_{13} , therefore resolving this degeneracy.

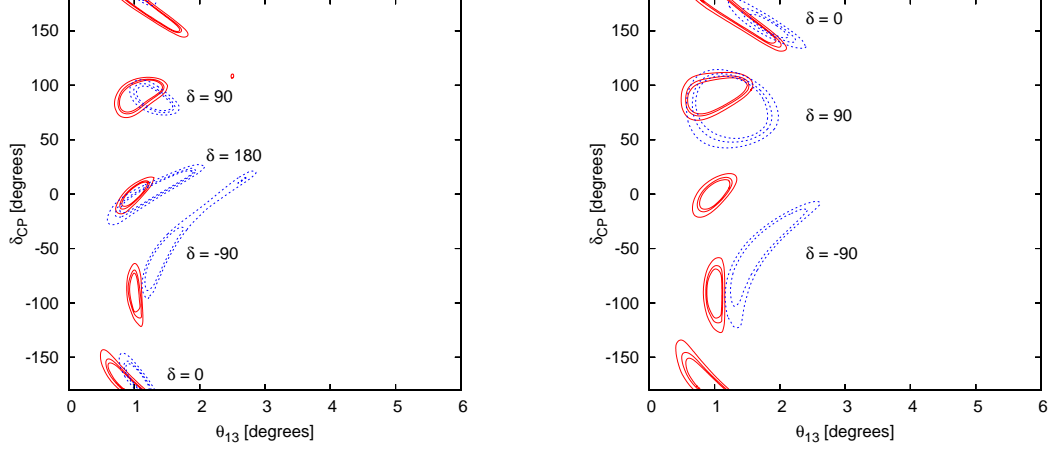


Figure 6: 90%, 95% and 99% CL contours for setup III-WC (left panel) and IV-WC (right panel), with solutions from discrete degeneracies included for $\theta_{13} = 1^\circ$, for different values of the CP-phase, $\delta = -90^\circ, 0^\circ, 90^\circ, 180^\circ$.

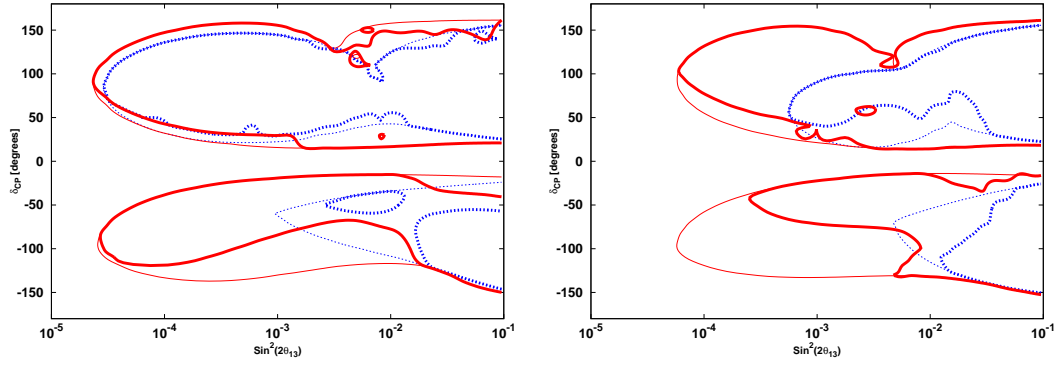


Figure 7: CP-violation discovery potential at 99% CL for setup III-WC (left panel) and IV-WC (right panel). In each case, we present the results for the beta-beam only (blue dotted lines) and the combination with the electron capture result (red solid lines), both without (thin lines) and with (thick lines) taking the hierarchy degeneracy into account.

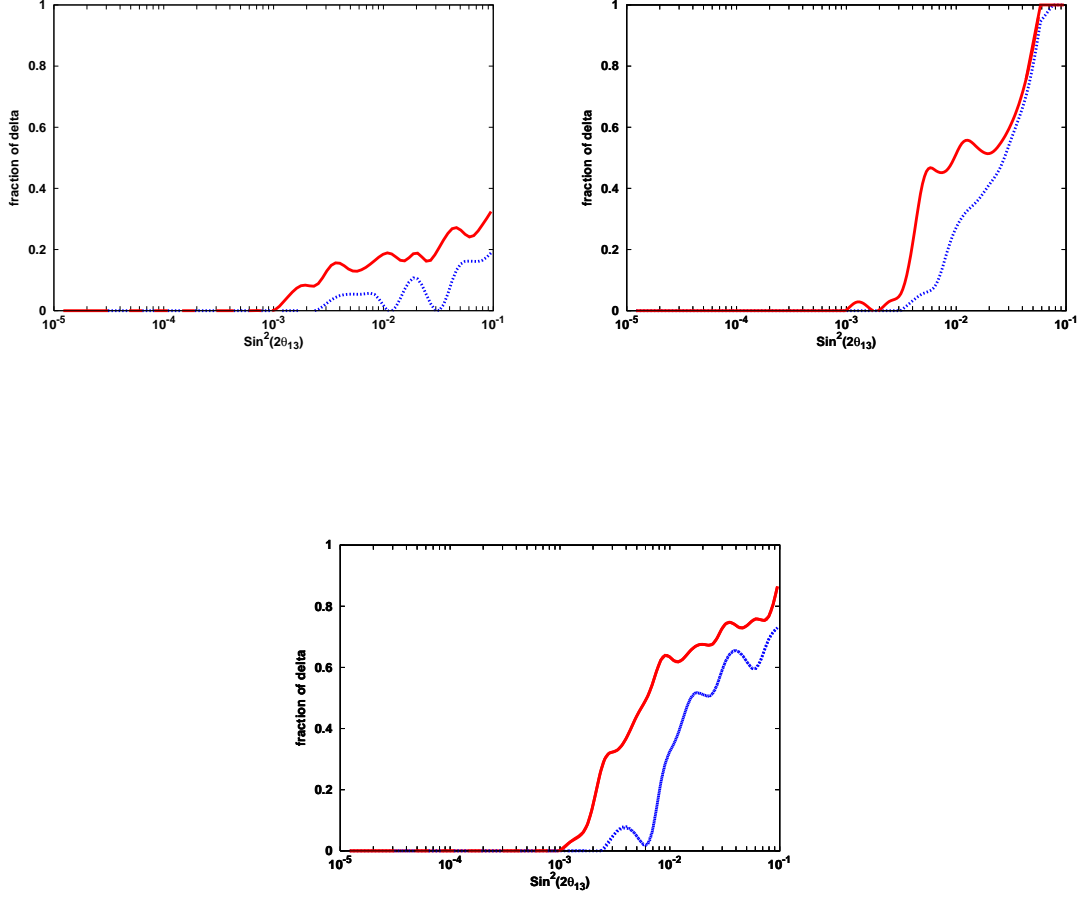


Figure 8: Fraction of δ for which the neutrino mass hierarchy can be determined at 99% CL for setup III-WC (left upper panel) and IV-WC (right upper panel), with present priors in the known parameters. The same fraction of δ is presented in the lower panel for setup III-WC with negligible errors in the known parameters. In each case, we present the results for the beta-beam only (blue dotted lines) and the combination with the electron capture result (red solid lines).

7. Mass hierarchy determination

In Fig. 8, we present the results for the neutrino mass hierarchy determination for the setups with a 0.5 Mton WC detector (setups III-WC and IV-WC). We do not consider the CERN-Frejus cases; the shorter baseline being unable to distinguish the type of hierarchy.

In both cases, the contribution from the beta-beam channel is shown in blue dashed lines and the result for the combination with the electron capture channel is shown by the red solid lines. As matter effects are more important at high energies, we see that the inclusion of the electron capture flux improves the results.

The CERN-Boulby baseline, with its larger matter effect, represents a much more promising setup for the determination of the mass hierarchy. Its resolution would be possible for all values of δ for $\sin^2 2\theta_{13} \simeq \text{few} \times 10^{-2}$, even for the present priors in the known parameters. The power of having negligible errors in the known parameters is presented for setup III-WC associated with the CERN-Canfranc baseline, showing a much higher fraction of δ for which the neutrino mass hierarchy can be determined.

8. Conclusions

We have exploited in this presentation the power of using different neutrino energies, in a unique experimental setup, in order to disentangle the CP-odd term in the interference between the atmospheric and solar amplitudes for the suppressed neutrino oscillation $P(\nu_e \rightarrow \nu_\mu)$. This strategy has been implemented by the use of a parent ion with two comparable channels of decay: electron capture (EC) and β^+ -decay (BB). The CP phase sensitivity is thus obtained by only using neutrinos, thanks to the Energy Dependence of the oscillation probability provided by the combination of the two EC and BB channels.

We found that the two separate channels EC and BB have a limited overlap of the allowed regions in the (θ_{13}, δ) plane, resulting in a good resolution of the intrinsic degeneracy. With the SPS upgrade to higher energy ($E_p = 1000 \text{ GeV}$), one gets a better sensitivity to CP-violation discovery and measurement, iff accompanied by a longer baseline of 600 km at least. This aim is the main focus for the third generation neutrino oscillation experiments.

The best E/L for higher sensitivity to the mixing $|U(e3)|$, typically the first oscillation maximum, is not the same than that for the CP phase determination. Like the phase-shift in a interference pattern, the effect of δ is easier to observe by going to the energy region of the second oscillation. This covering is obtained with the combination of the two EC and BB channels for the same ion and the same boost.

The setups III and III-WC, with a baseline $L = 650 \text{ km}$, have larger counting rates and a better tuning of the beam to the oscillatory pattern, resulting in a very good ability for disentangling the two parameters (θ_{13}, δ) . These setups provide the best sensitivity for CP-violation with positive values of δ .

For negative δ 's, the type of hierarchy cannot be still resolved for $L = 650 \text{ km}$. In going to setups IV and IV-WC, with a baseline $L = 1050 \text{ km}$, the determination of the mass hierarchy is better and one obtains a good reach to CP-violation for negative δ .

The general conclusion is that the combination of the two EC and BB channels from a single decaying ion and a fixed γ -boost achieves remarkable results for the discovery of CP-violation and the measurement of the CP-phase. This is a virtue of

the different energy dependence of the CP-odd term and the CP-even terms in the oscillation probability, and there is no need of performing separate experiments, with different systematics and counting rates, for neutrinos and antineutrinos.

9. Acknowledgements

It is a pleasure to acknowledge Milla for the magnificent event organized in Venise. We would like to thank many colleagues for discussions and clarifications and, particularly, to our collaborators J. Burguet-Castell, M. Lindroos, C. Orme, S. Palomares-Ruiz and S. Pascoli. This research has been funded by the Spanish MICINN Grant FPA2008-02878 and by the Generalitat Valenciana Grant PROMETEO 2088/004.

10. References

- 1) Y. Ashie *et al.* [Super-Kamiokande Collaboration], Phys. Rev. D **71** (2005) 112005 [arXiv:hep-ex/0501064]; J. Hosaka *et al.* [Super-Kamiokande Collaboration], neutrinos in Super-Kamiokande,” Phys. Rev. D **74** (2006) 032002 [arXiv:hep-ex/0604011]; H. Sekiya for the Super-Kamiokande Collaboration, arXiv:0810.0595 [astro-ph].
- 2) M. Ambrosio *et al.* [MACRO Collaboration], Eur. Phys. J. C **36** (2004) 323; M. C. Sanchez *et al.* [Soudan 2 Collaboration], Phys. Rev. D **68**, 113004 (2003) [arXiv:hep-ex/0307069].
- 3) Y. Fukuda *et al.* [Kamiokande Collaboration], Phys. Rev. Lett. **77** (1996) 1683; B. T. Cleveland *et al.*, Astrophys. J. **496** (1998) 505; W. Hampel *et al.* [GALLEX Collaboration], Phys. Lett. B **447** (1999) 127; J. N. Abdurashitov *et al.* [SAGE Collaboration], J. Exp. Theor. Phys. **95** (2002) 181 [Zh. Eksp. Teor. Fiz. **122** (2002) 211] [arXiv:astro-ph/0204245]; T. A. Kirsten [GNO Collaboration], Nucl. Phys. Proc. Suppl. **118** (2003) 33.
- 4) S. Fukuda *et al.* [Super-Kamiokande Collaboration], Phys. Lett. B **539** (2002) 179 [arXiv:hep-ex/0205075]. J. P. Cravens *et al.* [Super-Kamiokande Collaboration], Phys. Rev. D **78** (2008) 032002 [arXiv:0803.4312 [hep-ex]];
- 5) Q. R. Ahmad *et al.* [SNO Collaboration], Phys. Rev. Lett. **87** (2001) 071301 [arXiv:nucl-ex/0106015]; *ibid.* **89** (2002) 011301 [arXiv:nucl-ex/0204008]; and *ibid.* **89** (2002) 011302 [arXiv:nucl-ex/0204009]. S. N. Ahmed *et al.* [SNO Collaboration], Phys. Rev. Lett. **92** (2004) 181301 [arXiv:nucl-ex/0309004]; B. Aharmim *et al.* [SNO Collaboration], Phys. Rev. C **72** (2005) 055502 [arXiv:nucl-ex/0502021].
- 6) M. Apollonio *et al.* [CHOOZ Collaboration], Phys. Lett. B **466** (1999) 415 [arXiv:hep-ex/9907037]; M. Apollonio *et al.* [CHOOZ Collaboration], Eur. Phys. J. C **27** (2003) 331 [arXiv:hep-ex/0301017].

- 7) F. Boehm *et al.*, Phys. Rev. Lett. **84** (2000) 3764 [arXiv:hep-ex/9912050]; Phys. Rev. D **62** (2000) 072002 [arXiv:hep-ex/0003022]; and *ibid.* **64** (2001) 112001 [arXiv:hep-ex/0107009].
- 8) K. Eguchi *et al.* [KamLAND Collaboration], Phys. Rev. Lett. **90** (2003) 021802 [arXiv:hep-ex/0212021]; T. Araki *et al.* [KamLAND Collaboration], Phys. Rev. Lett. **94** (2005) 081801 [arXiv:hep-ex/0406035]. S. Abe *et al.* [KamLAND Collaboration], Phys. Rev. Lett. **100** (2008) 221803 [arXiv:0801.4589 [hep-ex]].
- 9) M. H. Ahn *et al.* [K2K Collaboration], Phys. Rev. D **74** (2006) 072003 [arXiv:hep-ex/0606032].
- 10) D. G. Michael *et al.* [MINOS Collaboration], Phys. Rev. Lett. **97** (2006) 191801 [arXiv:hep-ex/0607088]; P. Adamson *et al.* [MINOS Collaboration], arXiv:0806.2237 [hep-ex]; arXiv:0807.2424 [hep-ex].
- 11) T. Schwetz, M. Tortola and J. W. F. Valle, New J. Phys. **10** (2008) 113011 [arXiv:0808.2016 [hep-ph]]; M. C. Gonzalez-Garcia, arXiv:0901.2505 [hep-ph].
- 12) G. L. Fogli, E. Lisi, A. Marrone, A. Palazzo and A. M. Rotunno, Phys. Rev. Lett. **101**, 141801 (2008) [arXiv:0806.2649 [hep-ph]].
- 13) G. L. Fogli, these Proceedings.
- 14) A. Bandyopadhyay *et al.* [ISS Physics Working Group], arXiv:0710.4947 [hep-ph].
- 15) “Euro- ν : High Intensity Neutrino Oscillation Facility in Europe”, FP7-infrastructure-2007-1 project number 212372.
- 16) F. Ardellier *et al.* [Double Chooz Collaboration], arXiv:hep-ex/0606025. X. Guo *et al.* [Daya Bay Collaboration] hep-ex/0701029; S. B. Kim [RENO Collaboration], AIP Conf. Proc. **981** (2008) 205 [J. Phys. Conf. Ser. **120** (2008) 052025]; H. Nunokawa [Angra Neutrino Collaboration], AIP Conf. Proc. **981** (2008) 208.
- 17) Y. Hayato *et al.*, Letter of Intent, available at <http://neutrino.kek.jp/jhfnu/>.
- 18) D. S. Ayres *et al.* [NOvA Collaboration], hep-ex/0503053. FERMILAB-PROPOSAL-0929, March 21, 2005. Revised nova Proposal available at <http://www-nova.fnal.gov/NOvA-Proposal/Revised-NOvA-Proposal.html>.
- 19) V. Barger, P. Huber, D. Marfatia and W. Winter, Phys. Rev. D **76** (2007) 053005 [arXiv:hep-ph/0703029]; V. Barger *et al.*, arXiv:0705.4396 [hep-ph].
- 20) S. Geer, Phys. Rev. D **57** (1998) 6989 [Erratum-*ibid.* D **59** (1999) 039903] [arXiv:hep-ph/9712290] A. De Rújula, M. B. Gavela and P. Hernández, Nucl. Phys. B **547** (1999) 21 [arXiv:hep-ph/9811390]; V. Barger, S. Geer, R. Raja and K. Whisnant, Phys. Rev. D **62** (2000) 013004 [arXiv:hep-ph/9911524]; M. Freund, M. Lindner, S. T. Petcov and A. Romanino, Nucl. Phys. B **578** (2000) 27 [arXiv:hep-ph/9912457].
- 21) S. Geer, O. Mena and S. Pascoli, Phys. Rev. D **75**, 093001 (2007) [arXiv:hep-ph/0701258]; A. D. Bross, M. Ellis, S. Geer, O. Mena and S. Pascoli, Phys. Rev. D **77**, 093012 (2008) [arXiv:0709.3889 [hep-ph]].

- 22) P. Zucchelli, Phys. Lett. B **532** (2002) 166.
- 23) M. Mezzetto, J. Phys. G **29** (2003) 1781 [arXiv:hep-ex/0302005]; and *ibid.* **29** (2003) 1771.
- 24) P. I. Krastev and S. T. Petcov, Phys. Lett. B **205** (1988) 84; J. Arafune and J. Sato, Phys. Rev. D **55** (1997) 1653 [arXiv:hep-ph/9607437]; J. Bernab  , Proc. WIN'99, World Scientific (2000), p. 227, hep-ph/9904474; M. Freund, M. Lindner and A. Romanino, Nucl. Phys. B **562** (1999) 29 [arXiv:hep-ph/9903308].
- 25) J. Bernab   and M. C. Ba  uls, Nucl. Phys. Proc. Suppl. **87** (2000) 315 [arXiv:hep-ph/0003299].
- 26) A. Cervera *et al.*, Nucl. Phys. B **579** (2000) 17 [Erratum-*ibid.* B **593** (2001) 731] [arXiv:hep-ph/0002108].
- 27) E. K. Akhmedov, R. Johansson, M. Lindner, T. Ohlsson and T. Schwetz, JHEP **0404** (2004) 078 [arXiv:hep-ph/0402175].
- 28) M. C. Ba  uls, G. Barenboim and J. Bernab  , Phys. Lett. B **513** (2001) 391 [arXiv:hep-ph/0102184]; J. Bernab   and S. Palomares-Ruiz, hep-ph/0112002; and Nucl. Phys. Proc. Suppl. **110** (2002) 339 [arXiv:hep-ph/0201090].
- 29) J. Bernab  , S. Palomares-Ruiz, A. P  rez and S. T. Petcov, Phys. Lett. B **531** (2002) 90 [arXiv:hep-ph/0110071]; S. Palomares-Ruiz and J. Bernab  , Nucl. Phys. Proc. Suppl. **138** (2005) 398 [arXiv:hep-ph/0312038].
- 30) J. Bernab  , S. Palomares Ruiz and S. T. Petcov, Nucl. Phys. B **669** (2003) 255 [arXiv:hep-ph/0305152]; S. Palomares-Ruiz and S. T. Petcov, Nucl. Phys. B **712** (2005) 392 [arXiv:hep-ph/0406096]; S. T. Petcov and S. Palomares-Ruiz, hep-ph/0406106; S. T. Petcov and T. Schwetz, Nucl. Phys. B **740** (2006) 1 [arXiv:hep-ph/0511277].
- 31) J. Bernabeu, J. Burguet-Castell, C. Espinoza and M. Lindroos, JHEP **0512** (2005) 014 [arXiv:hep-ph/0505054]; Nucl. Phys. Proc. Suppl. **155** (2006) 222 [arXiv:hep-ph/0510278]; PoS **HEP2005** (2006) 182 [arXiv:hep-ph/0512297]; arXiv:hep-ph/0512299; PoS **HEP2005** (2006) 365; J. Bernabeu and C. Espinoza, arXiv:hep-ph/0605132; C. Espinoza, J. Bernabeu, J. Burguet-Castell and M. Lindroos, AIP Conf. Proc. **885** (2007) 89.
- 32) J. Bernabeu and C. Espinoza, Phys. Lett. B **664** (2008) 285 [arXiv:0712.1034 [hep-ph]]; arXiv:hep-ph/0612316; AIP Conf. Proc. **917** (2007) 24; J. Phys. Conf. Ser. **110** (2008) 082006 [arXiv:0710.5615 [hep-ph]].
- 33) J. Sato, Phys. Rev. Lett. **95** (2005) 131804 [arXiv:hep-ph/0503144].
- 34) M. Rolinec and J. Sato, JHEP **0708** (2007) 079 [arXiv:hep-ph/0612148].
- 35) J. Bernabeu, C. Espinoza, C. Orme, S. Palomares-Ruiz and S. Pascoli, arXiv:0902.4903 [hep-ph].
- 36) B. Rubio and W. Gelletly, Lect. Notes Phys. **764** (2009) 99.

- 37) J. Burguet-Castell, D. Casper, J. J. Gomez-Cadenas, P. Hernandez and F. Sanchez, Nucl. Phys. B **695** (2004) 217 [arXiv:hep-ph/0312068]; J. Burguet-Castell, D. Casper, E. Couce, J. J. Gomez-Cadenas and P. Hernandez, Nucl. Phys. B **725** (2005) 306 [arXiv:hep-ph/0503021].
- 38) M. R. Bhat, Nucl. Data Sheets **89** (2000) 797.
- 39) C. W. Reich, Nucl. Data Sheets **99** (2003) 753.
- 40) A. Algora *et al.*, Proc. XXXII Symposium on Nuclear Physics, Cocoyoc, Morelos, Mexico (2009); M. E. Estévez *et al.*, DPG Spring Meeting, Bochum, Germany (2009); A. Algora, E. Estévez and B. Rubio, *private communication*.
- 41) H. Keller *et al.*, Z. Phys. A **352** (1995) 1.
- 42) E. Nácher *et al.*, GSI Sci. Report 2001, 8.
- 43) M. Lindroos, *private communication*.